Digital Twin of the Mooring Line Tension for Floating Offshore Wind Turbines

Jake Walker, *Member, IEEE,* Andrea Coraddu, *Member, IEEE,*
Luca Oneto, *Member, IEEE,* and Stuart Kilbourn

***Abstract*—The number of installed Floating Offshore Wind Turbines (FOWTs) has doubled since 2017, quadrupling the total installed capacity, and is expected to increase significantly over the next decade. Consequently, there is a growing consideration towards the main challenges for FOWT projects: monitoring the system's integrity, extending the lifespan of the components, and maintaining FOWTs safely at scale. Effectively and efficiently addressing these challenges would unlock the wide-scale deployment of FOWTs. In this work, we focus on one of the most critical components of the FOWTs, the Mooring Lines (MoLs), which are responsible for fixing the structure to the seabed. The primary mechanical failure mechanisms in MoLs are extreme load and fatigue, both of which are functions of the axial tension. An effective solution to detect long term drifts in the mechanical response of the MoLs is to develop a Digital Twin (DT) able to accurately predict the behaviour of the healthy system to compare with the actual one. Authors will leverage operational data collected from the world's first commercial floating wind farm (Hywind Pilot Park[1]) in 2018, to investigate the effectiveness of the DT for the prediction of the MoL axial tension. The DT will be developed using state-of-the-art data-driven methods, and results based on real operational data will support our proposal.**

***Index Terms*—Floating Offshore Wind Turbines, Mooring Lines, Axial Tension, Digital Twins, Data-Driven Models**

I. Introduction

Floating Wind is one of the fastest-growing sectors within the Offshore Renewable Energy Industry and internationally recognised as one of the most promising renewable energy sources to satisfy a significant proportion of global energy demands [1]. The ability to economically deploy Floating Offshore Wind Turbines (FOWTs) in deepwater areas, that were previously unfeasible for development using fixed-bottom turbines, is one of the fundamental driving forces behind the success of Floating Wind [2]. In fact, deepwater areas are often characterised by higher average wind speeds and consequently an higher average capacity factors that could improve the economic viability of offshore wind energy [3]. However, Floating Wind is still an emerging market, and only a limited number of pilots have been deployed, so there is still a significant amount work required to address the unique aspects to Floating Wind: monitoring the system's integrity, extending the lifespan of the components, and maintaining FOWTs safely at scale [1], [2], [4]. Nevertheless, due to the success of Pilot FOWTs around the world, the industry is now focused on addressing these remaining challenges before deploying FOWTs at scale in deepwater [4]. In particular, the use, monitoring, and maintenance of the station-keeping devices (i.e., the Mooring Lines - MoLs) devoted to anchor the FOWT structure in place pose some of the most prominent challenges to overcome [4].

Experience from the Oil&Gas industry indicates that the demanding environmental conditions such as the corrosive salt-water and forceful waves, combined with the isolation of the deployment sites, are particularly damaging to the MoLs and may pose issues for checking and maintaining the integrity of FOWTs [5]. In addition, unlike Floating Production Storage and Offloading (FPSO) vessels, where there are typically between 12 and 24 MoLs, economic drivers within the renewables sector tend to produce designs with no redundancy [6]. For this reason, each MoL is critical to the FOWT structure, and failure is catastrophic [7]. Nevertheless, the extreme conditions in which MoLs operate call for regular inspections to prevent disastrous failures and downtime. Inspections are usually performed in two ways: close visual inspection by divers and through Remotely Operated Vehicles (ROVs) [8], being both options uneconomical [9]. For these reasons, within the Oil&Gas industry, alternative strategies for monitoring MoLs integrity are actually employed, like using load cell to detect rapid failure by extreme load [10] or using GPS-based devices (e.g., LifeLine JIP [11]) to detect an unusual excursion caused by the loss of a single mooring [11].

Regarding FOWT failures and maintenance activities, since this industry is in its infancy, there is very little publicly available data describing the expected failure rates of FOWTs or the required maintenance schedules [12]. According to [13] for a fixed-bottom offshore wind farm with 200 turbines, it may be necessary to perform up to $3,000$ maintenance visits per year. Since the mechanics of FOWTs are similar to the fixed-bottom turbines, it is safe to consider Floating Wind farms will require (at least) a similar number of maintenance visits. With this in mind, the ability to schedule maintenance by forecasting the health status of FOWTs becomes fundamental to deploy FOWTs maintenance at scale [14]. Similar considerations should also be made towards the safety of the maintenance operations. In fact, since a failure could be catastrophic [7], developing an early warning system able to predict a failure

Jake Walker and Andrea Coraddu - Department of Naval Architecture, Ocean and Marine Engineering, University of Strathclyde, Scotland (e-mail: jake.walker@strath.ac.uk, andrea.coraddu@strath.ac.uk).

Andrea Coraddu - Department of Maritime & Transport Technology, Delft University of Technology, The Netherlands (e-mail: a.coraddu@tudelft.nl).

Luca Oneto - DIBRIS, University of Genoa, Italy (e-mail: luca.oneto@unige.it).

Stuart Kilbourn - Fugro GB Marine Ltd., Glasgow Office (e-mail: s.killbourn@fugro.com).

[1]https://www.equinor.com/en/what-we-do/floating-wind/hywind-scotland.html

early enough to secure a safe working environment is essential to ensure the safety of maintenance operations.

In order to estimate the health conditions it is required to develop computational models of the mooring systems. Contrarily to visual inspections, computational models can ensure an economic, reliable, and effective monitoring tools for the integrity of the MoLs [15].

In the literature, it is possible to find a large body of work addressing MoL failures [16], [17], [8], [18], [19], [20], [21], [22], [23], [24], [25], [26], [27], [28], [29], [30]. The primary mechanical failure mechanisms in mooring systems are extreme load and fatigue, both of which are functions of the axial tension [17]. By exploiting this relationship, it is possible to use the MoL axial tension as an indicator for the health status of the Mooring System. In addition, [8] acknowledge MoL failures are often focused at the top of the chain, as these are the points of highest tension and the most stressed locations. The works available in the literature can be grouped into two main families: Physical Models (PMs) and Data-Driven Models (DDMs). PMs and DDMs can be used to detect long term drifts in the mechanical response of the MoLs by developing a Digital Twin (DT) able to accurately predict the behaviour of the healthy system to compare with the actual one. A DT is a specific type of model that embodies a precise digital copy of a physical system [31]. Consequently, DTs are an effective method of forecasting the future behaviour of a system after the DT has learned the behaviour from historical examples [32].

PMs are primarily based on the mechanistic knowledge of the MoLs behaviour. Authors of [21] provided a good overview of the mooring dynamics PMs considering their advantages and limitations, describing in details simple, approximate (linear force-displacement or force-displacement-velocity models), and high fidelity (finite-element approach) methods.

Instead, DDMs allow us to develop computationally aware real-time monitoring systems for MoLs by learning the input-output behaviour of a system from historical examples without any a-priori knowledge about the MoLs. DDMs require a single intensive learning phase (i.e., model construction) and benefit from a computationally inexpensive forward phase (i.e., model used as a predictor) [33], making them well suited to develop DTs. [26], [27], [28], [29] have all proposed using DDMs to monitor other marine energy systems (Floating platforms, FPSO vessels, etc.), and noted the potential for predictive models to reduce the cost of operational monitoring. In particular, [27] propose a DDM to approximate the MoL tension in place of a computationally expensive PM (specifically a Finite Element Analysis) by use of a non-linear autoregressive exogenous model. Fatigue damage of MoLs has been investigated by [30] using an Artificial Neural Network (ANN), where they observe the significant influence of the environmental conditions (waves, winds, and currents) on the tension bands. Additionally, [23], [34] demonstrate the potential benefits of using DDMs for FOWT MoLs when scaling health monitoring tools site-wide.

To the best of the authors' knowledge, no one has yet developed DTs of the FOWT MoLs to detect long-term drifts in the mechanical response. Moreover, the previous literature on monitoring FOWTs has been focused only on synthetic data and scenarios. Developing strategies to address these problems and testing the solutions with real data could provide the necessary information to address the outlined challenges sufficiently.

For these reasons, to detect long-term drifts in the mechanical response of the MoLs, we will develop a DT able to accurately predict the behaviour of the healthy system to compare with the actual one. The DT will be developed using state-of-the-art data-driven methods [35], [36] and results based on real operational data will support our proposal.

The rest of the paper is organised as follows. Section II summarises the problem we aim to address and the related available dataset. Section III describes the proposed modelling approach, based on DDMs, to address the problem summarised in Section II using the previously described dataset. Section IV reports the experimental results showing the effectiveness of our proposal. Finally, Section V concludes the paper.

II. Problem and Dataset Description

In this section we will summarise the problems under investigation and the available data that can be exploited for building models able to address them.

In this work, we aim to face the problem of detect long term drifts in the mechanical response of the MoLs. For this purpose, as described in Section I, we will develop a DT able to infer the expected behaviour of the MoLs in healthy conditions to compare with the actual one. Drifts in the differences between the actual and the predicted (healthy) behaviour is an indicator of decay in the condition of the MoL [37]. This DT will take as inputs the current status of the factors influencing the MoL behaviour (i.e., the motions of the turbine and the environmental conditions) and as output the MoL axial tension.

In order to develop our DT we will exploit the publicly available Hywind dataset [38]. The dataset describes the weather, motion, and mooring line axial tension of an SWT-6.0-154 turbine floating in depths of between 95-120m, 25 km off the coast of Scotland. The dataset is composed of 11 intervals of the turbine motion and response, in 30 minute windows over the course of 2018. Table I describes the features of the data set. Table II reports the data collection periods together and the key operational information (i.e., the significant wave height - H_s and the peak waves period - T_p). A schematic of the turbine and the relevant sensor placement is seen in Figure 1.

III. Proposed Approach

In the proposed context, predicting the axial tension of the FOWT MoLs, a general modelisation framework can be defined, characterised by an input space $\mathcal{X} \subseteq \mathbb{R}^d$, an output space $\mathcal{Y} \subseteq \mathbb{R}^b$, and an unknown relation $\mu : \mathcal{X} \rightarrow \mathcal{Y}$ to be learned [35], [39]. For what concerns this work, $\mathcal{X}$ is composed by the the motions of the turbine and the environmental conditions (i.e., D_e, D_n, θ_N, ϕ_N, θ_T, ϕ_T, ψ_T, v, and ψ_{dir} in Table I) while the output space $\mathcal{Y}$ refers to the

TABLE I: Hywind data set [38] features.

Variable Name	ID	Unit	Sampling Rate [Hz]
Date-Time	t	[s]	10
Drift (Easting)	D_e	[m]	10
Drift (Northing)	D_n	[m]	10
Nacelle Pitch	θ_N	[rad]	10
Nacelle Roll	ϕ_N	[rad]	10
Tower Pitch	θ_T	[rad]	10
Tower Roll	ϕ_T	[rad]	10
Tower Yaw	ψ_T	[rad]	1
Wind speed	v	$[\frac{\mathrm{m}}{\mathrm{s}}]$	10
Yaw Direction	ψ_{dir}	[°]	10
Tension Line 1 - Bridle 1	$T_{\mathrm{ML_1B_1}}$	[kN]	5
Tension Line 1 - Bridle 2	$T_{\mathrm{ML_1B_2}}$	[kN]	5
Tension Line 2 - Bridle 1	$T_{\mathrm{ML_2B_1}}$	[kN]	5
Tension Line 2 - Bridle 2	$T_{\mathrm{ML_2B_2}}$	[kN]	5
Tension Line 3 - Bridle 1	$T_{\mathrm{ML_3B_1}}$	[kN]	5
Tension Line 3 - Bridle 2	$T_{\mathrm{ML_3B_2}}$	[kN]	5

TABLE II: Hywind data set [38] data collection periods together and the key operational information.

Interval	Date-Time Range	H_s [m]	T_p [s]
1	2018-03-26 23:15 - 23:45	2.23	10.6
2	2018-01-14 15:25 - 15:55	4.21	8.7
3	2018-04-14 00:25 - 00:55	2.07	10.5
4	2018-02-13 01:05 - 01:35	2.13	6.5
5	2018-02-24 04:35 - 05:05	2.51	7.3
6	2018-01-09 09:25 - 09:55	3.25	9.3
7	2018-01-06 07:45 - 08:15	4.41	10.9
8	2018-07-29 03:45 - 04:15	3.02	7.85
9	2018-05-02 03:15 - 04:45	2.28	6.5
10	2018-01-24 11:15 - 11:45	3.87	8.3
11	2018-01-24 11:25 - 11:55	3.85	8.3

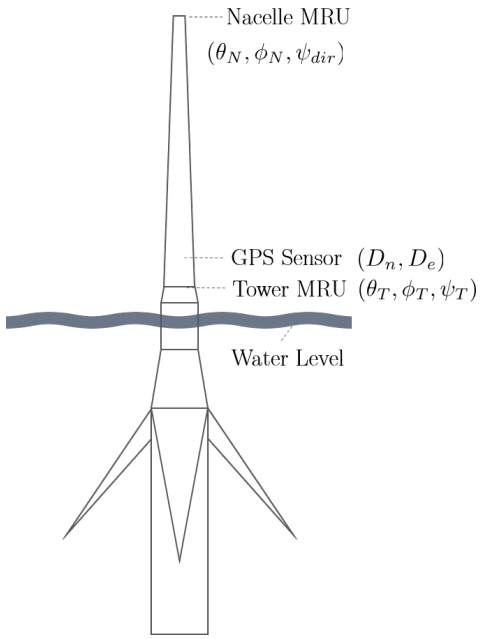

(a) Wind Turbine Tower.

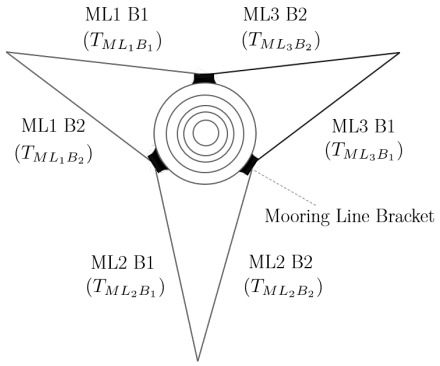

(b) Mooring Lines.

Fig. 1: Schematic of an FOWT including the relevant sensor placement for the features described in Table I.

axial tensions of the FOWT MoL bridles (i.e., $T_{\mathrm{ML_1B_1}}$, $T_{\mathrm{ML_1B_2}}$, $T_{\mathrm{ML_2B_1}}$, $T_{\mathrm{ML_2B_2}}$, $T_{\mathrm{ML_3B_1}}$, and $T_{\mathrm{ML_3B_2}}$ in Table I).

In this context, the authors define the model $h : \mathcal{X} \to \mathcal{Y}$ as an artificial simplification of μ. Now, the model h represents a DT of the FOWT MoL bridles. In our work, we aim to develop a DT (see Section II) to infer the expected behaviour of the MoLs in healthy conditions to compare with the actual one. Then the input space is composed by instantaneous information at time t (i.e., D_e, D_n, θ_N, ϕ_N, θ_T, ϕ_T, ψ_T, v, and ψ_{dir} in Table I) while the output space is the axial tensions of the FOWT MoL bridles at time t (i.e., $T_{\mathrm{ML_1B_1}}$, $T_{\mathrm{ML_1B_2}}$, $T_{\mathrm{ML_2B_1}}$, $T_{\mathrm{ML_2B_2}}$, $T_{\mathrm{ML_3B_1}}$, and $T_{\mathrm{ML_3B_2}}$ in Table I).

The model h, as described in Section I can be obtained with different kinds of techniques, for example, requiring some physical knowledge of the problem, as in PMs, or the acquisition of large amounts of data, as in DDMs. In this paper we will use a state-of-the-art DDM for the reasons described in Section I. Between the DDMs it is possible to identify two families of approaches [35], [40]. The first one, comprising traditional Machine Learning methods, needs an initial phase where the features must be defined a-priori from the data via feature engineering or implicit or explicit feature mapping [35], [41], [42]. The second family, which includes deep learning methods, automatically learns both the features and the models from the data [40]. For small cardinality datasets and outside particular applications (e.g., computer vision and natural language processing) Deep Learning does not perform well since they require huge amount of data to be reliable and to outperform traditional Machine Learning models [43], [44].

Machine Learning maps the problem of building the two DTs in a typical regression problem [45], [42]. In fact, ML techniques aim at estimating the unknown relationship μ between input and output through a learning algorithm $\mathscr{A}_{\mathcal{H}}$ which exploits some historical data to learn h and where $\mathcal{H}$ is a set of hyperparameters which characterises the generalisation performance of $\mathscr{A}$ [36]. The historical data consists on a series of n examples of the input/output relation μ and are defined as $\mathcal{D}_n = \{(\boldsymbol{x}_1, \boldsymbol{y}_1), \cdots, (\boldsymbol{x}_n, \boldsymbol{y}_n)\}$ where $\boldsymbol{x} \in \mathcal{X}$ and $\boldsymbol{y} \in \mathcal{Y}$. For simplicity we will indicate with y one of the elements in $\boldsymbol{y}$ since predicting a series of targets is equivalent to make a model for each one of the targets [35].

In this paper we will leverage on a Machine Learning model coming from the Kernel Methods family called Kernel Regularised Least Squares (KRLS) [46]. The idea behind KRLS can be summarised as follows. During the training phase, the quality of the learned function $h(\boldsymbol{x})$ is measured according to a loss function $\ell(h(\boldsymbol{x}), y)$ [47] with the empirical error

$$\hat{L}_n(h) = \frac{1}{n}\sum_{i=1}^{n} \ell(h(\boldsymbol{x}_i), y_i). \tag{1}$$

A simple criterion for selecting the final model during the training phase could then consist in simply choosing the approximating function that minimises the empirical error $\hat{L}_n(h)$. This approach is known as Empirical Risk Minimization (ERM) [45]. However, ERM is usually avoided in Machine Learning as it leads to severe overfitting of the model on the training dataset. As a matter of fact, in this case the training process could choose a model, complicated enough to perfectly describe all the training samples (including the noise, which afflicts them). In other words, ERM implies memorisation of data rather than learning from them. A more effective approach is to minimise a cost function where the trade-off between accuracy on the training data and a measure of the complexity of the selected model is achieved [48], implementing the Occam's razor principle

$$h^* : \quad \min_{h} \quad \hat{L}_n(h) + \lambda\, C(h). \tag{2}$$

In other words, the best approximating function h^* is chosen as the one that is complicated enough to learn from data without overfitting them. In particular, $C(\cdot)$ is a complexity measure: depending on the exploited Machine Learning approach, different measures are realised. Instead, $\lambda \in [0, \infty)$ is a hyperparameter, that must be set a-priori and is not obtained as an output of the optimisation procedure: it regulates the trade-off between the overfitting tendency, related to the minimisation of the empirical error, and the underfitting tendency, related to the minimisation of $C(\cdot)$. The optimal value for λ is problem-dependent, and tuning this hyperparameter is a non-trivial task, as will be discussed later in this section. In KRLS, models are defined as

$$h(\boldsymbol{x}) = \boldsymbol{w}^T \boldsymbol{\varphi}(\boldsymbol{x}), \tag{3}$$

where $\boldsymbol{\varphi}$ is an a-priori defined Feature Mapping (FM) [35] allowing to keep the structure of $h(\boldsymbol{x})$ linear. The complexity of the models, in KRLS, is measured as

$$C(h) = \|\boldsymbol{w}\|^2, \tag{4}$$

i.e., the Euclidean norm of the set of weights describing the regressor, which is a standard complexity measure in ML [35], [46]. Regarding the loss function, the square loss is typically adopted because of its convexity, smoothness, and statistical properties [47]

$$\hat{L}_n(h) = \frac{1}{n}\sum_{i=1}^{n} \ell(h(\boldsymbol{x}_i), y_i) = \frac{1}{n}\sum_{i=1}^{n} \left[h(\boldsymbol{x}_i) - y_i\right]^2. \tag{5}$$

Consequently, Problem (2) can be reformulated as

$$\boldsymbol{w}^* : \quad \min_{\boldsymbol{w}} \quad \sum_{i=1}^{n} \left[\boldsymbol{w}^T \boldsymbol{\varphi}(\boldsymbol{x}) - y_i\right]^2 + \lambda \|\boldsymbol{w}\|^2. \tag{6}$$

By exploiting the Representer Theorem [49], the solution h^* of the Problem (6) can be expressed as a linear combination of the samples projected in the space defined by $\boldsymbol{\varphi}$

$$h^*(\boldsymbol{x}) = \sum_{i=1}^{n} \alpha_i \boldsymbol{\varphi}(\boldsymbol{x}_i)^T \boldsymbol{\varphi}(\boldsymbol{x}). \tag{7}$$

It is worth underlining that, according to the kernel trick, it is possible to reformulate $h^*(\boldsymbol{x})$ without an explicit knowledge of $\boldsymbol{\varphi}$, and consequently avoiding the curse of dimensionality of computing $\boldsymbol{\varphi}$, by using a proper kernel function $K(\boldsymbol{x}_i, \boldsymbol{x}) = \boldsymbol{\varphi}(\boldsymbol{x}_i)^T \boldsymbol{\varphi}(\boldsymbol{x})$

$$h^*(\boldsymbol{x}) = \sum_{i=1}^{n} \alpha_i K(\boldsymbol{x}_i, \boldsymbol{x}). \tag{8}$$

Several kernel functions can be retrieved in literature [50], [51], each one with a particular property that can be exploited based on the problem under exam. Usually the Gaussian kernel is chosen

$$K(\boldsymbol{x}_i, \boldsymbol{x}) = e^{-\gamma \|\boldsymbol{x}_i - \boldsymbol{x}\|^2}, \tag{9}$$

because of the theoretical reasons described in [52], [53] and because of its effectiveness [43], [44]. γ is another hyperparameter, which regulates the nonlinearity of the solution that must be tuned as explained later. Basically the Gaussian kernel is able to implicitly create an infinite dimensional $\boldsymbol{\varphi}$ and thanks to this, the KRLS are able to learn any possible function [52]. The KRLS problem of Eq. (6) can be reformulated by exploiting kernels as

$$\boldsymbol{\alpha}^* : \quad \min_{\boldsymbol{\alpha}} \quad \|Q\boldsymbol{\alpha} - \boldsymbol{y}\|^2 + \lambda \boldsymbol{\alpha}^T Q \boldsymbol{\alpha}, \tag{10}$$

where $\boldsymbol{y} = [y_1, \ldots, y_n]^T$, $\boldsymbol{\alpha} = [\alpha_1, \ldots, \alpha_n]^T$, the matrix Q such that $Q_{i,j} = K(\boldsymbol{x}_j, \boldsymbol{x}_i)$, and the identity matrix $I \in \mathbb{R}^{n \times n}$. By setting the gradient equal to zero w.r.t. $\boldsymbol{\alpha}$ it is possible to state that

$$(Q + \lambda I)\, \boldsymbol{\alpha}^* = \boldsymbol{y}, \tag{11}$$

which is a linear system for which effective solvers have been developed over the years, allowing it to cope with even very large sets of training data [54].

The problems we still have to face is how to tune the hyperparameters for this approach (λ and γ) and how to estimate the performance of the final model. Model Selection (MS) and Error Estimation (EE) deal exactly with these problems [36]. Resampling techniques are commonly used by researchers and practitioners since they work well in most situations and this is why we will exploit them in this work [36]. Other alternatives exist, based on the Statistical Learning Theory, but they tend to underperform resampling techniques in practice [36]. Resampling techniques are based on a simple idea: the original dataset $\mathcal{D}_n$ is resampled once or many (n_r) times, with or without replacement, to build three

independent datasets called learning, validation and test sets, respectively $\mathcal{L}_l^r$, $\mathcal{V}_v^r$, and $\mathcal{T}_t^r$, with $r \in \{1, \cdots, n_r\}$ such that

$$\mathcal{L}_l^r \cap \mathcal{V}_v^r = \oslash, \quad \mathcal{L}_l^r \cap \mathcal{T}_t^r = \oslash, \quad \mathcal{V}_v^r \cap \mathcal{T}_t^r = \oslash \tag{12}$$

$$\mathcal{L}_l^r \cup \mathcal{V}_v^r \cup \mathcal{T}_t^r = \mathcal{D}_n \tag{13}$$

Subsequently, to select the best hyperparameters' combination $\mathcal{H} = \{\lambda, \gamma\}$ in a set of possible ones $\mathfrak{H} = \{\mathcal{H}_1, \mathcal{H}_2, \cdots\}$ for the algorithm $\mathscr{A}_\mathcal{H}$ or, in other words, to perform the MS phase, the following procedure has to be applied:

$$\mathcal{H}^* : \quad \arg\min_{\mathcal{H} \in \mathfrak{H}} \sum_{r=1}^{n_r} M(\mathscr{A}_\mathcal{H}(\mathcal{L}_l^r), \mathcal{V}_v^r), \tag{14}$$

where $h = \mathscr{A}_\mathcal{H}(\mathcal{L}_l^r)$ is a model built with the algorithm $\mathscr{A}$ with its set of hyperparameters $\mathcal{H}$ and with the data $\mathcal{L}_l^r$, and where $M(h, \mathcal{V}_v^r)$ is a desired metric. Since the data in $\mathcal{L}_l^r$ are independent from the data in $\mathcal{V}_v^r$, $\mathcal{H}^*$ should be the set of hyperparameters which allows achieving a small error on a data set that is independent from the training set. Then, to evaluate the performance of the optimal model which is $h^*_\mathscr{A} = \mathscr{A}_{\mathcal{H}^*}(\mathcal{D}_n)$ or, in other words, to perform the EE phase, the following procedure has to be applied:

$$M(h^*_\mathscr{A}) = \frac{1}{n_r} \sum_{r=1}^{n_r} M(\mathscr{A}_{\mathcal{H}^*}(\mathcal{L}_l^r \cup \mathcal{V}_v^r), \mathcal{T}_t^r). \tag{15}$$

Since the data in $\mathcal{L}_l^r \cup \mathcal{V}_v^r$ are independent from the ones in $\mathcal{T}_t^r$, $M(f^*_\mathscr{A})$ is an unbiased estimator of the true performance, measured with the metric M, of the final model [36]. In this work we will rely on Complete k-fold cross validation which means setting $n_r \leq \binom{n}{k}\binom{n-\frac{n}{k}}{k}$, $l = (k-2)\frac{n}{k}$, $v = \frac{n}{k}$, and $t = \frac{n}{k}$ and the resampling must be done without replacement [36].

For what concerns the metric M that we will use in our paper we will rely on the Mean Absolute Error (MAE) which computes the average absolute distance between the prediction and the actual value to predict [55]. Since in regression it is quite hard to synthesise the quality of a predictor in a single metric we will also rely on visualisation techniques like the scatter plot [56] (see Section IV).

IV. Experimental Results

This section is devoted to the presentation of the results of applying and testing the methodology described in Section III leveraging on the data presented in Section II.

As first step we have to report the hyperparameters ranges of the MS phase which is common to all experiments. The set of hyperparameters tuned during the MS phase is $\mathcal{H} = \{\gamma, \lambda\}$ chosen in $\mathfrak{H} = \{10^{-4.0}, 10^{-3.8}, \cdots, 10^{+4.0}\} \times \{10^{-4.0}, 10^{-3.8}, \cdots, 10^{+4.0}\}$. All of the tests have been repeated 30 times, and the average results are reported together with their t-student 95% confidence interval, to ensure the statistical validity of the results.

The proposed DT was designed to predict the MoL tension in healthy conditions to monitor the drift between the expected and true behaviour. This DT has to predict the instantaneous MoL tension from the current factors influencing the MoLs (i.e., the motions of the turbine and the environmental conditions) to accurately forecast the MoLs tension.

TABLE III: MAE for the different MoLs and bridles.

ML_1B_1	ML_1B_2	ML_2B_1	ML_2B_2	ML_3B_1	ML_3B_2
11.4±0.1	11.6±0.1	14.7±0.1	22.9±0.2	12.2±0.2	12.5±0.1

Table III reports the MAE for the different MoLs and bridles. Moreover Figure 2 reports the scatter plot (Real versus Predicted) the real distribution, and the error distribution for the axial tension of the different MoLs and bridles.

From Table III and Figure 2 it is possible to observe that the proposed DT is able to accurately predict the MoL tension in healthy conditions from the current factors influencing the MoLs (i.e., the motions of the turbine and the environmental conditions). In particular, with the exception of the ML_2B2 the MAE error for the remaining 5 bridles is under 15 [kN] across our tests as reported in Table III). At this point, it is important to remember that the dataset is composed of sporadic periods throughout the year (as described in Table II) and such captures a wide range of operating conditions (which is clear from the metocean features reported in the same table). Despite this wide range of operating conditions, the DTs exhibit small error variance indicating that the models performed consistently well across all conditions. Figure 2 allows us to better understand the quality of the developed DTs, further supporting the discussion raised from the tabular results, showing the behaviour of the predictions against the measured MoL tension by means of scatter plots and distributions of the measured MoL tension and errors. As one can observe from Figure 2 the DTs consistently performs well across the different MoLs and bridles. Based on these results we can safely state that the family of DTs we developed in this section would be well suited for monitoring the health status of the MoLs by detecting drifts between the expected MoL tension and the real one.

V. Conclusions

The number of installed FOWTs has exponentially grown in the last decade, quadrupling the total installed capacity. This growth is expected to continue in the next decade leading to an increasing need to address main challenges for FOWT projects: monitoring the system's integrity, extending the lifespan of the components, and maintaining FOWTs safely at scale. Effectively and efficiently addressing these challenges would unlock the wider-scale deployment of FOWTs.

For these reasons, in this work, we developed a DTs to predict the MoL tension of a FOWT exploiting state-of-the-art data-driven methods and leveraging the data coming from the Hywind Pilot Park to test our proposals. The proposed DT was able to predict the MoL tension under healthy conditions to monitor the drift between the expected and true behaviour. This DT represents an effective solution to detect long term drifts in the mechanical response of the MoLs, and accurately predict the behaviour of the healthy system to compare with the actual one.

As a concluding remark, it is important to stress that this work is just a preliminary step forward validated on a limited

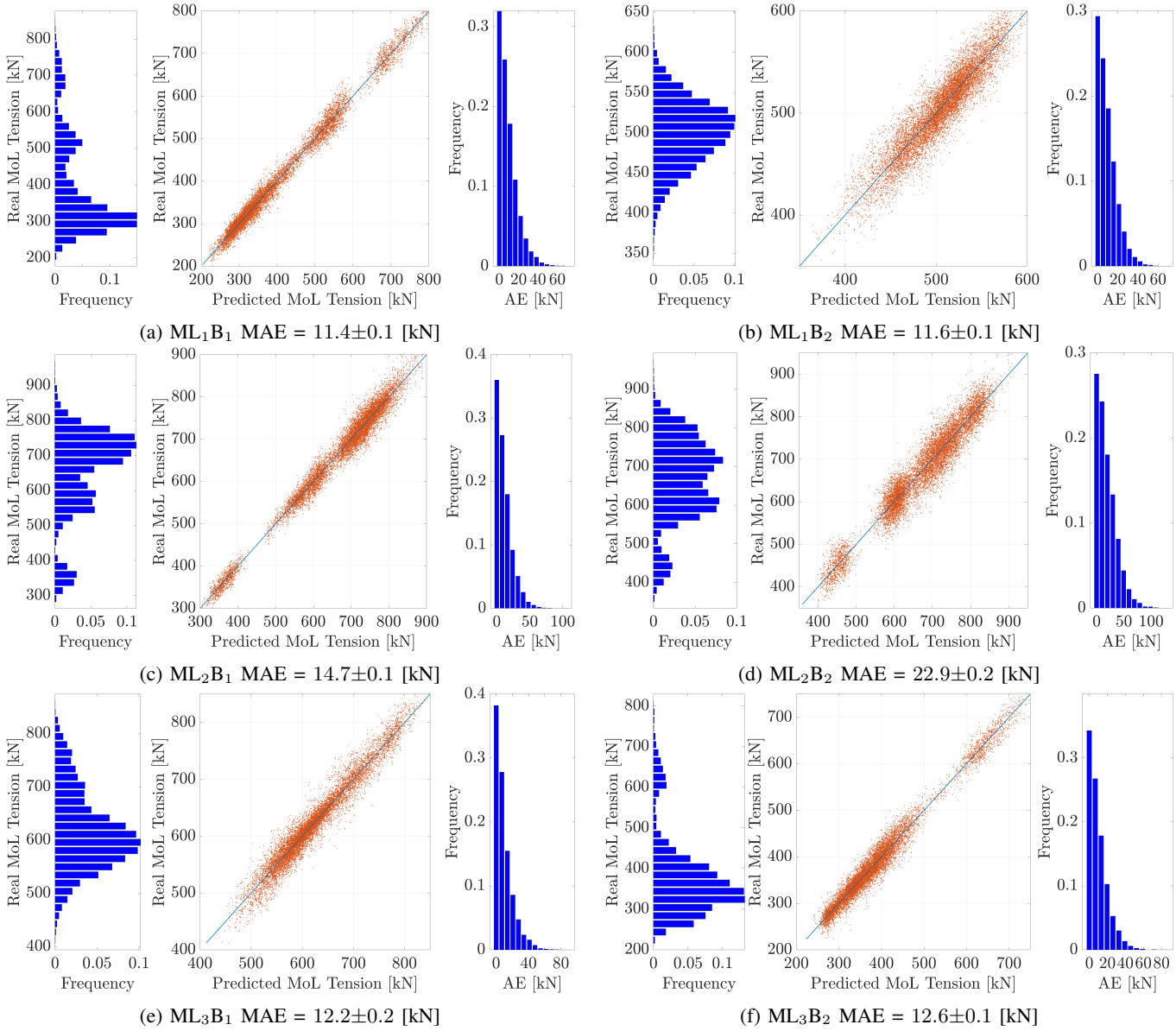

(a) ML_1B_1 MAE = 11.4±0.1 [kN]

(b) ML_1B_2 MAE = 11.6±0.1 [kN]

(c) ML_2B_1 MAE = 14.7±0.1 [kN]

(d) ML_2B_2 MAE = 22.9±0.2 [kN]

(e) ML_3B_1 MAE = 12.2±0.2 [kN]

(f) ML_3B_2 MAE = 12.6±0.1 [kN]

Fig. 2: Scatter plot (Real versus Predicted) the real distribution, and the error distribution for the axial tension of the different MoLs and bridles.

amount of data. The commercial use of FOWTs is still in its infancy, and the available dataset only captures sporadic periods throughout the year. For this reason, more tests with a more extensive set of data need to be conducted. Moreover, these DTs need to be integrated into real monitoring, control, and safety systems to validate the potentiality of the models.

REFERENCES

[1] Carbon Trust, "Market and Technology Review," in *Floating Offshore Wind*, 2015.

[2] ——, "Phase 1 Summary Report," in *Floating Wind Joint Industry Project*, 2018.

[3] M. Hannon, E. Topham, J. Dixon, D. McMillan, and M. Collu, *Offshore wind, ready to float? Global and UK trends in the floating offshore wind market*. University of Strathclyde, 2019.

[4] Carbon Trust, "Phase 2 summary report," in *Floating Wind Joint Industry Project*, 2020.

[5] S. Butterfield, W. Musial, J. Jonkman, P. Sclavounos, and L. Wayman, "Engineering challenges for floating offshore wind turbines," in *2005 Copenhagen Offshore Wind Conference*, 2007.

[6] Fugro N.V., "Fugro GB Marine Ltd." https://www.fugro.com/, 2020.

[7] G. Ma, L. Zhong, X. Zhang, Q. Ma, and H. S. Kang, "Mechanism of mooring line breakage of floating offshore wind turbine under extreme coherent gust with direction change condition," *Journal of Marine Science and Technology (Japan)*, vol. 25, 2020.

[8] M. G. Brown, T. D. Hall, D. G. Marr, M. English, and R. O. Snell, "Floating production mooring integrity JIP - Key findings," in *Annual Offshore Technology Conference*, 2005.

[9] ABSG Consulting, "Study on Mooring System Integrity Management for Floating Structures," https://www.bsee.gov/sites/bsee.gov/files/tap-technical-assessment-program//730-aa.pdf, 2015.

[10] P. Lu, "On The Monitoring Of Mooring System Performance," in *21st SNAME Offshore Symposium*, 2016.

[11] Marin LifeLine, "Dry Mooring Line Monitoring for Floating Production Systems," https://www.marin.nl/jips/lifeline, 2021.

[12] F. P. Santos, A. P. Teixeira, and C. Guedes Soares, "Operation and maintenance of floating offshore wind turbines," in *Floating Offshore Wind Farms*, 2016.

[13] C. Röckmann, S. Lagerveld, and J. Stavenuiter, "Operation and maintenance costs of offshore wind farms and potential multi-use platforms in the dutch north sea," in *Aquaculture Perspective of Multi-Use Sites in the Open Ocean: The Untapped Potential for Marine Resources in the Anthropocene*, 2017.

[14] Z. Ren, A. S. Verma, Y. Li, J. J. Teuwen, and Z. Jiang, "Offshore wind turbine operations and maintenance: A state-of-the-art review," *Renewable and Sustainable Energy Reviews*, vol. 144, 2021.

[15] Á. Angulo, G. Edwards, S. Soua, and T.-H. Gan, "Mooring Integrity Management: Novel Approaches Towards In Situ Monitoring," *Structural Health Monitoring - Measurement Methods and Practical Applications*, 2017.

[16] K. Ma, H. Shu, P. Smedley, D. L´Hostis, and A. Duggal, "A Historical Review on Integrity Issues of Permanent Mooring Systems," in *Offshore Technology Conference*, 2013.

[17] J. Davidson and J. V. Ringwood, "Mathematical modelling of mooring systems for wave energy converters - A review," *Energies*, vol. 10, no. 5, p. 666, 2017.

[18] M. K. Al-Solihat and M. Nahon, "Flexible multibody dynamic modeling of a floating wind turbine," *International Journal of Mechanical Sciences*, vol. 142-143, pp. 518–529, 2018.

[19] J. A. Aranha and M. O. Pinto, "Dynamic tension in risers and mooring lines: An algebraic approximation for harmonic excitation," *Applied Ocean Research*, vol. 23, no. 2, pp. 63–81, 2001.

[20] M. A. Bhinder, M. Karimirad, S. Weller, Y. Debruyne, M. Guérinel, and W. Sheng, "Modelling mooring line non-linearities (material and geometric effects) for a wave energy converter using AQWA, SIMA and Orcaflex," in *European Wave and Tidal Energy Conference*, 2015.

[21] M. Borg, M. Collu, and A. Kolios, "Offshore floating vertical axis wind turbines, dynamics modelling state of the art. Part II: Mooring line and structural dynamics," *Renewable and Sustainable Energy Reviews*, vol. 39, pp. 1226–1234, 2014.

[22] W. T. Hsu, K. P. Thiagarajan, M. Hall, M. MacNicoll, and R. Akers, "Snap loads on mooring lines of a floating offshore wind turbine structure," in *Proceedings of the International Conference on Offshore Mechanics and Arctic Engineering*, 2014.

[23] W. T. Hsu, K. P. Thiagarajan, M. MacNicoll, and R. Akers, "Prediction of extreme tensions in mooring lines of a floating offshore wind turbine in a 100-year Storm," in *International Conference on Offshore Mechanics and Arctic Engineering*, 2015.

[24] C. Jin and M. Kim, "Time-Domain Hydro-Elastic Analysis of a SFT (Submerged Floating Tunnel) with Mooring Lines under Extreme Wave and Seismic Excitations," *Applied Sciences*, vol. 8, p. 2386, 2018.

[25] D. Qiao, J. Yan, H. Liang, D. Ning, B. Li, and J. Ou, "Analysis on snap load characteristics of mooring line in slack-taut process," *Ocean Engineering*, vol. 196, p. 106807, 2020.

[26] S. Maroju, K. Delaney, C. Leon, and I. Prislin, "Estimation of critical platform integrity parameters in the absence of direct measurements in the context of integrated marine monitoring systems," in *International Conference on Ocean, Offshore and Arctic Engineering*, 2013.

[27] A. C. de Pina, A. A. de Pina, C. H. Albrecht, B. S. Leite Pires de Lima, and B. P. Jacob, "ANN-based surrogate models for the analysis of mooring lines and risers," *Applied Ocean Research*, vol. 41, pp. 76–86, 2013.

[28] I. Prislin and S. Maroju, "Mooring integrity and machine learning," in *Proceedings of the Annual Offshore Technology Conference*, 2017.

[29] V. Jaiswal and A. Ruskin, "Mooring line failure detection using machine learning," in *Proceedings of the Annual Offshore Technology Conference*, 2019.

[30] C. B. Li, J. Choung, and M. H. Noh, "Wide-banded fatigue damage evaluation of Catenary mooring lines using various Artificial Neural Networks models," *Marine Structures*, vol. 60, pp. 186–200, 2018.

[31] L. Oneto, A. Coraddu, F. Cipollini, O. Karpenko, K. Xepapa, P. Sanetti, and D. Anguita, "Crash Stop Maneuvering Performance Prediction:

[34] W. T. Hsu, K. P. Thiagarajan, and L. Manuel, "Extreme mooring tensions due to snap loads on a floating offshore wind turbine system," *Marine Structures*, vol. 55, pp. 182–199, 2017.

a Data-Driven Solution for Safety and Collision Avoidance," *Data-Enabled Discovery and Applications*, vol. 2, no. 1, pp. 1–11, 2018.

[32] A. Coraddu, L. Oneto, D. Ilardi, S. Stoumpos, and G. Theotokatos, "Marine dual fuel engines monitoring in the wild through weakly supervised data analytics," *Engineering Applications of Artificial Intelligence*, vol. 100, p. 104179, 2021.

[33] A. Coraddu, L. Oneto, F. Cipollini, and M. Kalikatzarakis, "Physical , Data-Driven , and Hybrid Approaches to Model Engine Exhaust Gas Temperatures in Operational Conditions," *Ships and Offshore Structures*, 2020.

[35] S. Shalev-Shwartz and S. Ben-David, *Understanding machine learning: From theory to algorithms*. Cambridge university press, 2014.

[36] L. Oneto, *Model Selection and Error Estimation in a Nutshell*. Springer, 2020.

[37] A. Coraddu, . Oneto, F. Baldi, F. Cipollini, M. Atlar, and S. Savio, "Data-driven ship digital twin for estimating the speed loss caused by the marine fouling," *Ocean Engineering*, vol. 186, p. 106063, 2019.

[38] Catapult ORE, "Floating turbine design cases," 2020. [Online]. Available: https://pod.ore.catapult.org.uk/data-collection/floating-turbine-design-cases

[39] J. D. Hamilton, *Time series analysis*. Princeton university press, 1994.

[40] I. Goodfellow, Y. Bengio, and A. Courville, *Deep Learning*. MIT Press, 2016.

[41] A. Zheng and A. Casari, *Feature engineering for machine learning: principles and techniques for data scientists*. O'Reilly Media, Inc., 2018.

[42] J. Shawe-Taylor and N. Cristianini, *Kernel methods for pattern analysis*. Cambridge university press, 2004.

[43] M. Fernández-Delgado, E. Cernadas, S. Barro, and D. Amorim, "Do we need hundreds of classifiers to solve real world classification problems?" *The journal of machine learning research*, vol. 15, no. 1, pp. 3133–3181, 2014.

[44] M. Wainberg, B. Alipanahi, and B. J. Frey, "Are random forests truly the best classifiers?" *The Journal of Machine Learning Research*, vol. 17, no. 1, pp. 3837–3841, 2016.

[45] V. N. Vapnik, *Statistical learning theory*. Wiley New York, 1998.

[46] V. Vovk, "Kernel ridge regression," in *Empirical inference*, 2013.

[47] L. Rosasco, E. De Vito, A. Caponnetto, M. Piana, and A. Verri, "Are loss functions all the same?" *Neural Computation*, vol. 16, no. 5, pp. 1063–1076, 2004.

[48] A. N. Tikhonov and V. Y. Arsenin, *Methods for solving ill-posed problems*. Nauka, Moscow, 1979.

[49] B. Schölkopf, R. Herbrich, and A. J. Smola, "A generalized representer theorem," in *Computational learning theory*, 2001.

[50] B. Scholkopf, "The kernel trick for distances," in *Advances in neural information processing systems*, 2001, pp. 301–307.

[51] N. Cristianini and J. Shawe-Taylor, *An introduction to support vector machines and other kernel-based learning methods*. Cambridge university press, 2000.

[52] S. S. Keerthi and C. J. Lin, "Asymptotic behaviors of support vector machines with gaussian kernel," *Neural computation*, vol. 15, no. 7, pp. 1667–1689, 2003.

[53] L. Oneto, A. Ghio, S. Ridella, and D. Anguita, "Support vector machines and strictly positive definite kernel: The regularization hyperparameter is more important than the kernel hyperparameters," in *IEEE International Joint Conference on Neural Networks (IJCNN)*, 2015.

[54] D. M. Young, *Iterative solution of large linear systems*. DoverPublications, 2003.

[55] C. J. Willmott and K. Matsuura, "Advantages of the mean absolute error (mae) over the root mean square error (rmse) in assessing average model performance," *Climate research*, vol. 30, no. 1, pp. 79–82, 2005.

[56] L. Shao, A. Mahajan, T. Schreck, and D. J. Lehmann, "Interactive regression lens for exploring scatter plots," in *Computer Graphics Forum*, 2017.